IET Smart Grid

Research Article

IET Journals
The Institution of Engineering and Technology

Distributed voltage and frequency synchronisation control scheme for islanded inverter-based microgrid

eISSN 2515-2947
Received on 22nd February 2018
Revised 14th May 2018
Accepted on 26th June 2018
E-First on 18th July 2018
doi: 10.1049/iet-stg.2018.0020
www.ietdl.org

Sonam Shrivastava[1], Bidyadhar Subudhi[1] ✉, Susmita Das[1]

[1]Department of Electrical Engineering, National Institute of Technology Rourkela, Centre for Renewable Energy Systems, Rourkela 769008, Orissa, India

✉ *E-mail: bidyadhar@nitrkl.ac.in*

Abstract: This study presents a fully distributed control paradigm for secondary control of islanded AC microgrid (MG). The proposed method addresses both voltage and frequency restoration for inverter-based distributed generators (DGs). The MG system has droop controlled DG units with predominantly inductive transmission lines and different communication topologies. The restoration scheme is fully distributed in nature, and the DGs need to communicate with their neighbours using a sparse communication network. The proposed control scheme is efficient to provide quick restoration of the voltage and frequency whilst accurate power-sharing is achieved despite disturbances. Further, convergence and stability analysis of the proposed control scheme is presented. The proposed algorithm avoids the need for a central controller and complex communication structure thereby reducing the computational burden and the risk of single-point-failure. The performance of the proposed control scheme has been verified considering variations in load and communication topologies and link delay by pursuing an extensive simulation study in MATLAB/SimPowerSystem toolbox. The proposed control scheme supports plug-and-play demand and scalability of MG network. The proposed control scheme is also compared with the neighbourhood tracking error based distributed control scheme and observed that the former exhibit faster convergence and accurate performance despite disturbances in MG network.

1 Introduction

In the modern era of smart power systems, the microgrid (MG) technology has been manifested as one of the promising technologies to facilitate the integration of renewable energy sources (RESs) into an existing power grid [1–3]. These RESs such as photovoltaic (PV), wind generators (WGs) and microturbines (MTs) are small-scale distributed generators (DGs) that are connected to the main grid network via voltage source inverters (VSIs) [4]. The physical characteristics of these inverter based-DGs are entirely different from the conventional synchronous generators (SGs). Hence there is a need for designing distinct control techniques for the above scenario. For instance, the SGs have large rotation mass and inertia which are coupled with the grid frequency for ensuring grid stability. However, in the case of DGs, the absence of inertia and rotating mass poses technical challenges such as the need for storage capacity and appropriate control action to ensure stability. A cluster of the DGs, loads, and energy storage units forms a locally controllable entity in the main grid and known as MG. The MG can operate in both grid-connected and islanded modes. MG is located close to the loads, and deliver electrical power with minimum losses and allow different RESs to connect in a distributed manner, hence provide better supply security. In a conventional power system, the grid forming units are synchronous generators, and they provide operating voltage and frequency for the whole network. Similarly, in grid-connected mode, main grid governs the operating voltage and frequency of the overall system, whereas, in an islanded mode of operation, these functions have to be provided by the VSI. Thus, control of the VSI becomes more complex and challenging [5, 6].

To synchronise the voltage and frequency of an islanded MG with the main grid, various hierarchical control structures have been presented in [7–10]. It is a three-layer control which comprises of primary, secondary and tertiary control levels. The primary control is realised locally via the droop control method at each DG terminal to maintain the voltage and frequency stability. Irrespective of the distributed nature of the droop control, it has a drawback of producing voltage and frequency deviations from their nominal values. Hence, the secondary control level is necessary to nullify the deviations caused by primary droop control and to restore the voltage and frequency to their nominal values. The tertiary control level works on the optimisation of the operating cost and power flow of the MG [11].

To overcome the drawbacks of primary control, secondary control is deployed. Traditionally, the secondary control level is implemented in a centralised manner [7, 10], which brings in the concept of global control action determined based on the information collected from the MG system. It also necessitates the use of a complicated two-way communication network and a central computing system, which impairs the reliability of the MG system. As a result, there is a risk of single-point-failure for the entire MG system. However, in recent studies, [12–14], distributed control of multi-agent system has evolved as a feasible solution to the problems associated with the centralised control structure. The distributed control structure only needs information of neighbouring DGs. Hence, the DG units communicate with each other using a sparse communication network. Without necessitating a central computing unit, the distributed secondary control scheme reduces the risk of single-point-failure and thus improves the system reliability. For a multi-agent system, considering each DG as an agent, the secondary voltage and frequency synchronisation becomes a consensus problem [15].

Recently, several distributed secondary control strategies have been reported in the literature [12, 15–26]. The majority of the approaches are based on consensus protocol [15, 22–25], where the agents reach consensus on the quantity of interest by using the exchanged information over a sparse communication network [27]. Parlak *et al.* [12] propose a frequency restoration scheme for a distributed power system with two un-interruptible power supply units. The scheme exploits a simple integral controller to restore the frequency in ∼28 s (not suitable for sensitive load), whereas the voltage regulation is not addressed. The control approach reported in [21, 24] address only frequency restoration via distributed averaging proportional integral controller, but needs centralised communication structure despite its decentralised implementation. In [28], a secondary frequency restoration scheme is presented with

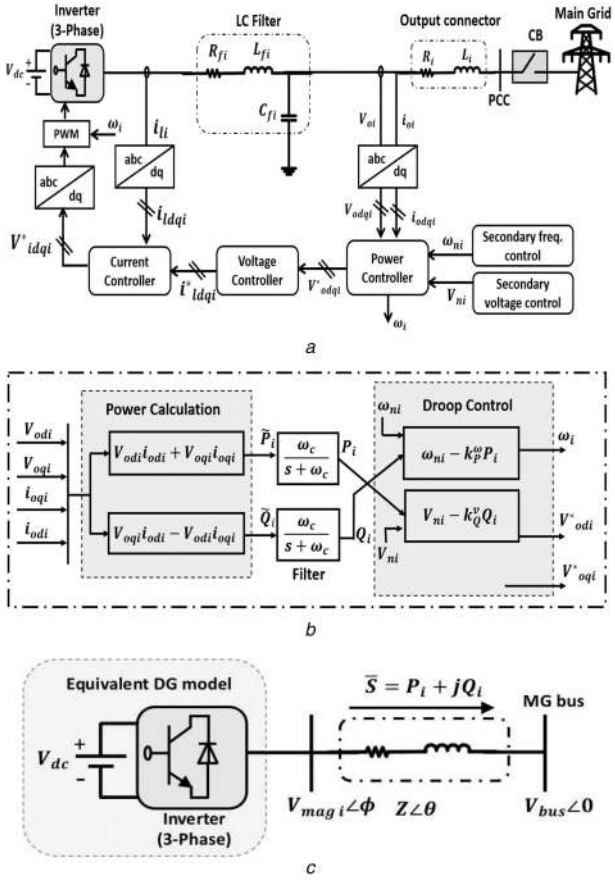

Fig. 1 *Modelling of DG*

a Dynamical model of inverter-based DG

b Block diagram of a power controller

c Equivalent model of DG connected to an MG bus

model predictive and smith predictor based controllers which employ a centralised complex communication structure. The secondary control scheme in [18] uses feedback linearisation to convert the secondary voltage restoration problem into a tracking synchronisation problem and uses a sparse communication structure. Schiffer *et al.* [19] provide a consensus-based voltage and reactive power regulation scheme and frequency restoration is not addressed. Further, the algorithm replaces the droop controller and makes the system prone to communication link failure. Shafiee *et al.* [25] present a team-oriented adaptive droop control scheme with dynamic consensus-based secondary control scheme only for voltage restoration. The distributed control approaches addressed in [15, 17, 22] deal with both voltage and frequency restoration, but need the detailed model of the MG system. However, DGs line, loads and MG configurations are unknown in practice, and the selection of controller gains are based on the algebraic connectivity of the communication network [27].

The consensus-based multi-agent control algorithm has been employed in different areas, including synchronous generators-based MG and inverter-based MG [20]. For accurate power sharing of multiple double-fed induction generators, the average consensus algorithm has been employed in [29]. A consensus-based algorithm is proposed to achieve power supply–demand balance in an islanded MG in [30]. Shafiee *et al.* [31] provide a distributed control approach for both voltage and frequency regulation but it uses the information of all DG units present in the MG network and necessitates a complex connected two-way communication network. Nasirian *et al.* [23] present a global voltage and reactive power regulation scheme based on a droop-free control methodology. The absence of droop mechanism can deteriorate the controller performance if the communication network breakdown occurs. Multi-functional distributed control framework is presented in [32] with voltage, frequency, and active power regulator module but needs normalised power information of all DGs present in MG. Dehkordi *et al.* [33] propose fully distributed cooperative secondary voltage and frequency restoration scheme, the control law is not independent of the MG system parameters.

This paper presents a fully distributed voltage and frequency restoration scheme which uses the sparse communication network while considering single integrator dynamics of DG with dominant inductive transmission lines. The MG is considered as a multi-agent system where each DG serves as an agent. The contributions of the paper can be summarised as follows:

- A fully distributed voltage and frequency synchronisation control algorithm is proposed for arbitrary electrical topology. Also, exponentially fast convergence and stability proofs for the proposed restoration algorithm are derived.
- Unlike the other distributed method that necessitates detailed knowledge of the MG system configuration in the proposed method, controller parameters do not depend on the MG line and load specifications and use only the local and neighbour information shared over a sparse communication network. This avoids the need for a central computing unit and complex communication network and provides a more reliable and efficient control framework.
- In comparison with the conventional distributed controller in [17], the proposed method achieves consensus rapidly and exhibits more accurate performance under controller activation and sudden load change and communication link delay. Also, the proposed method is fully independent of the line impedance and other DG parameters.

The remaining of this paper is organised as follows. In Section 2, we introduce a DG model and primary droop-based control scheme. Section 3 discusses the preliminaries of graph theory and the proposed distributed secondary control scheme for voltage and frequency synchronisation schemes of AC MG system. Simulation results and analysis are presented in Section 4. The paper is concluded in Section 5.

2 Modelling of DG

In an MG system, each DG unit comprises of a primary DC power source, a VSI, an LC filter and output connector as depicted in Fig. 1*a*. The detailed mathematical model of an inverter-based DG is introduced and analysed in [34]. The local primary control loops are power, voltage and current control loops which adjust the output voltage and frequency of the VSI [17, 18, 34]. The voltage and current control loops employ proportional–integral (PI) controllers. The power controller is modelled using real and reactive power droop techniques. The primary control deals with the voltage and frequency instability after islanding process, where the power generated does not match with the consumer's power demand. The droop control is an independent control method which eliminates the communication link requirement at the primary control level. A simplified model for power flow from an inverter to the MG is given in Fig. 1*c*. By neglecting high switching frequency harmonics, a DG can be modelled as an AC power source of $V_{\text{magi}}\angle\phi$. The bus voltage is assumed to be $V_{\text{bus}}\angle 0$ and lumped line impedance is represented as $Z\angle\theta$.

The complex power delivered from *i*th DG to the MG bus can be expressed as follows [35]:

$$\bar{S} = \bar{V}_{\text{bus}} \cdot \bar{I}^{*} = V_{\text{bus}}\angle 0 \cdot \left(\frac{V_{\text{magi}}\angle\phi - V_{\text{bus}}\angle 0}{Z\angle\theta}\right) = P_i + \text{j}Q_i \quad (1)$$

Separating the real and imaginary parts of $\bar{S}$ using Euler's formula, the real power (P_i) and reactive power (Q_i) for the *i*th DG can be obtained as follows:

$$\begin{aligned} P_i &= \frac{V_{\text{bus}} \cdot V_{\text{magi}}}{Z}\cos(\theta - \phi) - \frac{V_{\text{bus}}^2}{Z}\cos(\theta) \\ Q_i &= \frac{V_{\text{bus}} \cdot V_{\text{magi}}}{Z}\sin(\theta - \phi) - \frac{V_{\text{bus}}^2}{Z}\sin(\theta) \end{aligned} \quad (2)$$

For a typical MG, the resistance to inductance ratio depends on the line impedance and is smaller for a highly inductive transmission line [36, 37, 38, 39], $\theta = 90^{\circ}$, then (2) can be rewritten as

$$P_i = \frac{V_{\text{bus}} \cdot V_{\text{magi}}}{Z}\sin(\phi)$$
$$Q_i = \frac{V_{\text{bus}} \cdot V_{\text{magi}}}{Z}\cos(\phi) - \frac{V_{\text{bus}}^2}{Z} \tag{3}$$

If the phase difference ϕ between the inverter output voltage and MG bus voltage is small, then, $\sin\phi \simeq \phi$ and $\cos\phi \simeq 1$. Then (3) can be rewritten as

$$P_i \cong \frac{V_{\text{bus}} \cdot V_{\text{magi}}}{Z}\phi$$
$$Q_i \cong \frac{V_{\text{bus}} \cdot V_{\text{magi}} - V_{\text{bus}}^2}{Z} \tag{4}$$

which gives the linear relationship between (P_i, ϕ) and (Q_i, V_{magi}). Thus, voltage and frequency droop characteristics can be used to tune the voltage and frequency of inverter based on the following equations [40]:

$$V_{\text{magi}} = V_{ni} - k_Q^V Q_i \tag{5}$$

$$\omega_i = \omega_{ni} - k_P^{\omega} P_i \tag{6}$$

where ω_i is the angular frequency, V_{magi} is the magnitude of the output voltage. V_{ni} and ω_{ni} are the root mean square voltage and angular frequency of the ith DG at no load, i.e. reference values, respectively. k_Q^v and k_P^{ω} are the droop coefficients for the voltage and frequency control, respectively. The dynamics of each DG is derived in its own direct-quadrature $(d-q)$ reference frame. The primary controller provides the direct and quadratic terms of the reference voltage V_{odi}^* and V_{oqi}^* for the voltage control loop and operating angular frequency ω_i for the VSI. The block diagram of the power control loop is given in Fig. 1*b*. The low-pass filter with cut-off frequency ω_c is used to obtain the measured values of active and reactive power P_i and Q_i from the instantaneous values $\tilde{P}_i$ and $\tilde{Q}_i$ delivered by ith DG as follows:

$$P_i = \frac{\omega_c}{s + \omega_c}\tilde{P}_i$$
$$Q_i = \frac{\omega_c}{s + \omega_c}\tilde{Q}_i \tag{7}$$

The differential equation for the power controller can be given as [34]

$$\dot{Q}_i = -\omega_c Q_i + \omega_c\left(V_{oqi} i_{odi} - V_{odi} i_{oqi}\right) \tag{8}$$

$$\dot{P}_i = -\omega_c P_i + \omega_c\left(V_{odi} i_{odi} + V_{oqi} i_{oqi}\right) \tag{9}$$

where $\dot{P}_i$ and $\dot{Q}_i$ denote the time derivative of the active and reactive power, respectively. The primary controller is designed such that the output voltage magnitude is aligned with the direct component of the output voltage and quadratic term of the output voltage is set to zero

$$V_{odi}^* = V_{ni} - k_Q^V Q_i$$
$$V_{oqi}^* = 0 \tag{10}$$

It is clear from the droop control law in (5), and (6), that output voltage magnitude and frequency deviates from their nominal values if there is any change in the active and reactive power demand. Thus, appropriate secondary control strategies need to be designed for both voltage, and frequency synchronisation. The control objectives for an islanded MG are as follows:

- To synchronise the voltages of all DG units to their nominal values, i.e. $\lim_{t\to\infty} V_i(t) = V_{\text{nom}}, \quad \forall i \in N$, where N is the number of DGs.
- To synchronise the frequency of all DG units to their nominal values, i.e. $\lim_{t\to\infty} \omega_i(t) = \omega_{\text{nom}}, \quad \forall i \in N$.

It is worth mentioning that the synchronisation of V_{magi} is equivalent to the synchronisation of V_{odi}^* as

$$V_{\text{magi}} = \sqrt{V_{odi}^2 + V_{oqi}^2} = V_{odi}^* \tag{11}$$

3 Distributed secondary synchronisation scheme

This section first introduces the concept of the distributed control algorithm, which is further exploited in controller design for the proposed secondary voltage and frequency restoration scheme. The secondary control selects appropriate primary control references V_{ni} and ω_{ni} for voltage and frequency synchronisation, respectively. Low bandwidth communication links are required for information sharing between interconnected DGs, which can be implemented using wireless networks or power line communication. The MG is considered as a multi-agent system with each DG serves as an agent. These agents can exchange information with their neighbours by using a sparse communication network. Consider a weighted undirected graph also known as digraph defined as $G = (\mathcal{V}, \varepsilon, \mathcal{A})$ with N nodes (agents) $\mathcal{V} = \{1, \ldots, N\}$, $\varepsilon \subset \mathcal{V} \times \mathcal{V}$ is a set of edges (communication links), and the weighted adjacency matrix $\mathcal{A} = [a_{ij}] \in \mathcal{R}^{N\times N}$. If for all $(i, j) \in \varepsilon$ and $(j, i) \in \varepsilon$, then G is undirected, else it is called as a directed graph. The elements $a_{ij} = a_{ji} = 1$ if $j \subset N_i$, otherwise $a_{ij} = a_{ji} = 0$, the adjacency matrix $\mathcal{A}$ is a symmetric matrix. The set of neighbours of the node i is denoted as $N_i = \{j \in \mathcal{V} : (i, j) \in \varepsilon,\ j \neq i\}$. An edge from i to j, denoted as (i, j), means that agent j can send information to the agent i and vice versa. The Laplacian matrix of G is defined as $\mathcal{L} = \boldsymbol{D} - \mathcal{A}$, where $\boldsymbol{D}$ is called as in-degree matrix and defined as $\boldsymbol{D} = \text{diag}\{d_i\}$ where $d_i = \sum_{j\in N_i} a_{ij}$. $\mathcal{L}$ has all row sum equals to zero, i.e. $\mathcal{L}\mathbf{1}_N = 0$, where $\mathbf{1}_N$ is a vector of ones with length N. Based on the design of $\mathcal{L}$ at least one of the eigenvalues of $\mathcal{L}$ is zero and all other have positive real parts [41].

3.1 Distributed control algorithm

Considering a network with N agents having single integrator dynamics given as follows:

$$\dot{x}_i = u_i, \quad i \in \{1, \ldots, N\} \tag{12}$$

where $x_i \in \mathcal{R}$ is the ith agent state for agreement, i.e. voltage or frequency and $u_i \in \mathcal{R}$ is the control law. As explained earlier, the MG network is modelled as a weighted undirected graph G. The agent $i \in \{1, \ldots, N\}$ has access to the reference input signal $r_i \in \mathcal{R}$. To achieve the consensus amongst all agent's state following is the distributed algorithm [42]:

$$\dot{x}_i = \dot{r}_i - \alpha(x_i - r_i) - \beta\sum_{j=1}^{N}\mathcal{L}x_j - v_i$$
$$\dot{v}_i = \alpha\beta\sum_{j=1}^{N}\mathcal{L}x_j \tag{13}$$

where for $i \in \{1, \ldots, N\}$ x_i and v_i are the variables associated with the ith agent. $\mathcal{L}$ is the Laplacian matrix of the considered weighted digraph G. The first two terms cause the agents to move towards the reference input signal r_i, i.e. either reference voltage or frequency. The third and fourth terms comprise of PI feedback to force the consensus amongst the neighbouring agents. For a fixed topology on the communication network, this scheme results in

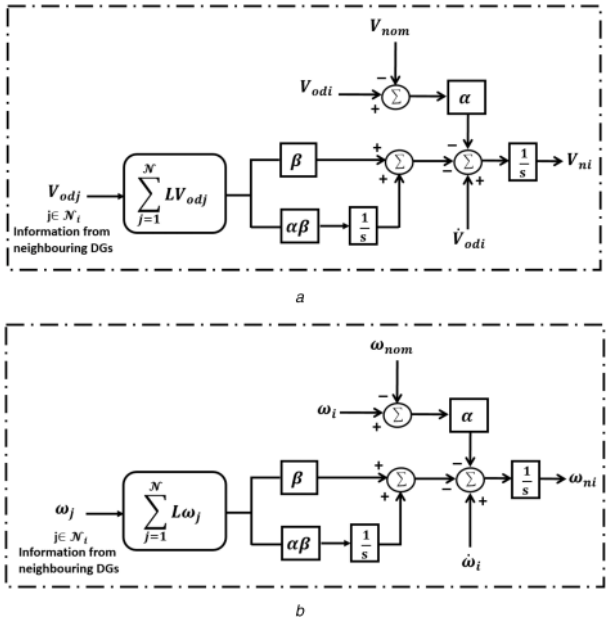

Fig. 2 *Modelling of DG*
a Proposed voltage synchronisation scheme
b Proposed frequency synchronisation scheme

each agent achieving consensus with the reference input across the network. The constants α and β are the design specifications which can be adjusted to achieve better performance.

3.2 Distributed secondary voltage synchronisation

Differentiating (5) we can write

$$\dot{V}^*_{odi} = \dot{V}_{ni} - k^V_Q \dot{Q}_i \tag{14}$$

$$\dot{V}_{ni} = \dot{V}^*_{odi} + k^V_Q \dot{Q}_i \tag{15}$$

The secondary voltage control reference input V_{ni} for primary droop control can be given as

$$V_{ni} = \int \left(\dot{V}^*_{odi} + k^v_Q \dot{Q}_i\right) \mathrm{d}t \tag{16}$$

Based on the distributed algorithm explained in Section 3.1, here a voltage synchronisation scheme has been proposed. For an inverter-based DG, single integrator dynamics for voltage magnitude can be represented as [19]

$$\dot{V}^*_{odi} = u^V_i \tag{17}$$

where $u^V_i : \mathcal{R} \geq 0 \rightarrow \mathcal{R}$ is the control input. For the ith DG, the proposed distributed-based secondary control can be given as

$$\begin{aligned} u^V_i &= \dot{V}_{\text{nom}} - \alpha(V^*_{odi} - V_{\text{nom}}) - \beta \sum_{j=1}^{N} \mathcal{L} V^*_{odj} - v^V_i \\ \dot{v}^V_i &= \alpha\beta \sum_{j=1}^{N} \mathcal{L} V^*_{odj} \end{aligned} \tag{18}$$

where V_{nom} is the nominal input reference voltage, $\mathcal{L}$ is the Laplacian matrix, and (α, β) are the design specifications. From (18), it is noted that the DG output voltage magnitude will synchronise to its nominal value for all DGs in the MG system, i.e. $V_{\text{magi}} \rightarrow V_{\text{nom}}$. The block diagram of the proposed secondary voltage synchronisation is shown in Fig. 2*a*. The proposed algorithm in (18) can be written in compact form as follows:

$$\dot{\boldsymbol{Y}} = \alpha \boldsymbol{Y} - \beta \mathcal{L} \boldsymbol{Y} - \boldsymbol{W}, \tag{19}$$

$$\dot{\boldsymbol{W}} = \alpha\beta \mathcal{L} \boldsymbol{Y} - \boldsymbol{\Pi}_N (\ddot{\boldsymbol{r}} + \alpha \dot{\boldsymbol{r}}) \tag{20}$$

where $\boldsymbol{\Pi}_N = \mathbf{I}_N - (1/N)\mathbf{1}_N \mathbf{1}_N^T$

$$y_i = x_i - \frac{1}{N} \sum_{j=1}^{N} r_j, i \in \{1, \ldots, N\} \tag{21}$$

$$\boldsymbol{W} = \boldsymbol{v} - \bar{\boldsymbol{v}}, \quad \bar{\boldsymbol{v}} = \boldsymbol{\Pi}_N (\dot{\boldsymbol{r}} + \alpha \boldsymbol{r}) \tag{22}$$

x_i is the ith agent's state for agreement. The zero system of (19) and (20) can be written as

$$\begin{bmatrix} \dot{\boldsymbol{Y}} \\ \dot{\boldsymbol{W}} \end{bmatrix} = \boldsymbol{A} \begin{bmatrix} \boldsymbol{Y} \\ \boldsymbol{W} \end{bmatrix}, \quad \text{where } \boldsymbol{A} = \begin{bmatrix} -\alpha \mathbf{I}_N - \beta \mathcal{L} & -\mathbf{I}_N \\ \alpha\beta \mathcal{L} & 0 \end{bmatrix} \tag{23}$$

Lemma 1: For any initial condition $Y(0), W(0) \in \mathcal{R}^N$, there exist any $\alpha, \beta > 0$ such that, the trajectory of (23) over the weighted balanced digraph satisfies [41]

$$y_i(t) \rightarrow \frac{\alpha^{-1}}{N} \sum_{j=1}^{N} W_j(0),$$

$$W_i(t) \rightarrow \frac{1}{N} \sum_{j=1}^{N} W_j(0), \text{ as } t \rightarrow \infty, \quad \forall i \in \{1, \ldots, N\}, \tag{24}$$

exponentially fast.

Proof: Consider the following variables change with $\boldsymbol{m} = (1/\sqrt{N})\mathbf{1}_N$ and $\boldsymbol{M}$ are such that $\boldsymbol{m}^T \boldsymbol{M} = 0$ and $\boldsymbol{M}^T \boldsymbol{M} = \mathbf{I}_{N-1}$,

$$\begin{bmatrix} \boldsymbol{p} \\ \boldsymbol{q} \end{bmatrix} = \boldsymbol{T}_1 \boldsymbol{T}_2 \begin{bmatrix} \boldsymbol{Y} \\ \boldsymbol{W} \end{bmatrix} \tag{25}$$

where

$$\boldsymbol{T}_1 = \begin{bmatrix} \mathbf{I}_N & 0 \\ \alpha \mathbf{I}_N & \mathbf{I}_N \end{bmatrix}, \quad \boldsymbol{T}_2 = \begin{bmatrix} \boldsymbol{T}_3^T & 0 \\ 0 & \boldsymbol{T}_3^T \end{bmatrix}, \quad \boldsymbol{T}_3 = [\boldsymbol{m} \quad \boldsymbol{M}]$$

We define new variables $\boldsymbol{p}$ and $\boldsymbol{q}$ as $\boldsymbol{p} = (p_1, \boldsymbol{p}_{2:N})$ and $\boldsymbol{q} = (q_1, \boldsymbol{q}_{2:N})$, where $p_1, q_1 \in \mathcal{R}$ and $\boldsymbol{p}_{2:N}, \boldsymbol{q}_{2:N} \in \mathcal{R}^{N-1}$. Using (25), (7) can be reformulated as follows:

$$\begin{bmatrix} \dot{p}_1 \\ \dot{q}_1 \end{bmatrix} = \tilde{\boldsymbol{A}} \begin{bmatrix} p_1 \\ q_1 \end{bmatrix}, \quad \tilde{\boldsymbol{A}} = \begin{bmatrix} 0 & -1 \\ 0 & -\alpha \end{bmatrix} \tag{26}$$

$$\begin{bmatrix} \dot{\boldsymbol{p}}_{2:N} \\ \dot{\boldsymbol{q}}_{2:N} \end{bmatrix} = \bar{\boldsymbol{A}} \begin{bmatrix} \boldsymbol{p}_{2:N} \\ \boldsymbol{q}_{2:N} \end{bmatrix}, \quad \bar{\boldsymbol{A}} = \begin{bmatrix} -\beta \boldsymbol{M}^T \mathcal{L} \boldsymbol{M} & -\mathbf{I}_{N-1} \\ 0 & -\alpha \mathbf{I}_{N-1} \end{bmatrix} \tag{27}$$

The eigenvalues of a matrix $\tilde{\boldsymbol{A}}$ are 0 and α. The eigenvalues of $\bar{\boldsymbol{A}}$ are α, with a multiplicity of $N-1$ and $\beta\lambda_i$, with $i \in \{2, \ldots, N\}$ where λ_i are eigenvalues of the Laplacian matrix $\mathcal{L}$. For the strongly connected weighted graph G, $\lambda_1 = 0$ and all other eigenvalues have positive real parts. Therefore, for $\alpha, \beta > 0$, the system (26) and (27) is stable and likewise (23) is also a linear stable system. For convergence property, consider the null space of a matrix $\boldsymbol{A}$ is given by $(\mathbf{1}_N, -\alpha \mathbf{1}_N)$, i.e. eigenvector associated with zero eigenvalues. Therefore, (23) achieves consensus with an exponentially fast rate to set

$$\{(\boldsymbol{Y}, \boldsymbol{W}) | \boldsymbol{Y} = \mu \mathbf{1}_N, \ \boldsymbol{W} = -\mu\alpha \mathbf{1}_N, \mu \in \mathcal{R}\} \tag{28}$$

Now, left multiplying (23) by $\mathrm{diag}\left(\mathbf{0}_N^T, \mathbf{1}_N^T\right)$ and using the weight-balance property of directed graph we get, $\sum_{i=1}^{N} \dot{W}_i = 0$, therefore

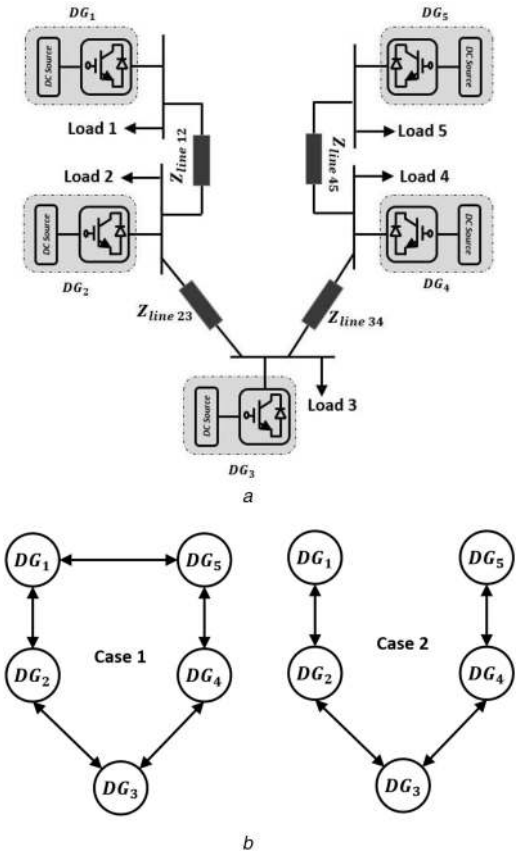

Fig. 3 *Communication structure for studied MG test system*
a Block diagram of the islanded MG test system
b Communication topology for cases 1 and 2

$$\sum_{i=1}^{N} W_i(t) = \sum_{i=1}^{N} W_i(0), \quad \forall, t \geq 0 \tag{29}$$

The combination of (28) and (29) yields that, from any initial condition $\boldsymbol{Y}(0)$, $\boldsymbol{W}(0) \in \mathscr{R}^N$, the path of (23) satisfies (24) with exponentially fast convergence. This completes the proof. □

Thus, the agreement state of an agent, i.e. the output voltage of DG will synchronise to the nominal value with (18). Proper selection of design specification α, β results in better performance. Usually, these parameters are chosen to be adequately large to achieve fast consensus amongst the DGs.

3.3 Distributed secondary frequency synchronisation

On differentiating (6), one obtains

$$\dot{\omega}_i = \dot{\omega}_{ni} - k_P^{\omega} \dot{P}_i \tag{30}$$

$$\dot{\omega}_{ni} = \dot{\omega}_i + k_P^{\omega} \dot{P}_i \tag{31}$$

The secondary voltage control reference input ω_{ni} for primary droop control can be given as

$$\omega_{ni} = \int \left(\dot{\omega}_i + k_P^{\omega} \dot{P}_i\right) \mathrm{d}t \tag{32}$$

For an inverter-based DG, single integrator dynamics for operating angular frequency can be represented as [19]

$$\dot{\omega}_i = u_i^{\omega} \tag{33}$$

where $u_i^{\omega}: \mathscr{R} \geq 0 \rightarrow \mathscr{R}$ is the control input. Based on the distributed control algorithm in (13) and the single integrator dynamics of the ith DG in (33), the secondary frequency synchronisation scheme can be given as

$$u_i^{\omega} = \dot{\omega}_{\text{nom}} - \alpha(\omega_i - \omega_{\text{nom}}) - \beta \sum_{j=1}^{N} \mathscr{L}\omega_j - v_i^{\omega} \tag{34}$$

$$\dot{v}_i^{\omega} = \alpha\beta \sum_{j=1}^{N} \mathscr{L}\omega_j \tag{35}$$

where ω_{nom} is the nominal input reference frequency, $\mathscr{L}$ is the Laplacian matrix and (α, β) are the design specifications. Using (34), the frequency can be synchronised to its nominal value for all DGs in MG system, i.e. $\omega_i \rightarrow \omega_{\text{nom}}$. The stability and convergence proofs are similar to (19)–(29) and can be omitted here. The block diagram of proposed distributed secondary frequency synchronisation is shown in Fig. 2*b*.

3.4 Communication network for secondary control

An evident feature of the proposed control scheme is its low bandwidth communication requirement among interconnected DG units. This local communication network provides information flow and can be implemented using a sparse communication network. For an MG in a small geographical area, power line communication is feasible, and if the physical structure of MG is known, it is easy to obtain a digraph with spanning tree which optimally connects all DG units. In conventional centralised control structure, if the communication link between the DG and the central controller breaks, the secondary control fails to operate, whereas in the proposed distributed control structure due to the loss of one communication link, the secondary control of DGs will not fail.

4 Results and discussion

The MG structure is shown in Fig. 3*a* is considered to verify the performance of the proposed secondary synchronisation scheme. The islanded MG (380 V, 50 Hz) is simulated for three different cases using MATLAB/SimPowerSystem toolbox. The studied MG test system is comprised of five DG units. The loads and transmission lines are modelled as series *RL* branches. The details of DGs and transmission lines are given in Tables 1 and 2. Table 3 gives loads of the MG test system. The parameters K_{PV}, K_{IV}, K_{PC} and K_{IC} denote the proportional and integral constants of PI-based voltage and current controllers. The parameters of the secondary controller are set as $\alpha = 3$, and $\beta = 10$. The simulation study is pursued four cases as follows. In case 1, the performance of the proposed control scheme is verified. In case 2, the proposed control scheme has been evaluated with different communication network topologies. In case 3, the proposed control scheme is compared with the method reported in [17]. In case 4, the proposed synchronisation scheme is evaluated with different communication latencies.

4.1 Case 1: Performance evaluation of controller

The performance of the proposed control scheme has been verified for sudden load change. The communication topology used in this case is shown in Fig. 3*b*, case 1. The following four stages are considered in a simulation study:

- *Stage 1:* At $t = 0$ s only primary droop control is active.
- *Stage 2:* At $t = 1.5$ s secondary voltage synchronisation scheme in (18) and frequency synchronisation scheme in (34) are activated.
- *Stage 3:* At $t = 2.5$ s load 1 is increased.
- *Stage 4:* At $t = 3.5$ s load 3 is removed.

Fig. 4 shows that in stage 1, only primary control was active and it causes the voltage and frequency to deviate from their nominal values. When the proposed secondary schemes in (18) and

Table 1 Specification of MG test system

Parameter	DG 1, DG 2 and DG 3	DG 4 and DG 5
V_{ref}	380 V	380 V
f_{ref}	50 Hz	50 Hz
k_P^V	9.4×10^{-5}	12.5×10^{-5}
k_P^ω	1.3×10^{-3}	1.5×10^{-3}
R	0.03 Ω	0.03 Ω
L	0.35 mH	0.35 mH
R_{f}	0.1 Ω	0.1 Ω
L_{f}	1.35 mH	1.35 mH
C_{f}	50 μF	50 μF
K_{PV}	0.1	0.05
K_{IV}	420	390
K_{PC}	15	10.5
K_{IC}	20,000	16,000
ω_{c}	31.41 rad/s	31.41 rad/s

Table 2 MG lines

	$Z_{\text{Line 12}}$	$Z_{\text{Line 23}}$	Z_{Line34}	Z_{Line45}
lines	$R_l = 0.12\,\Omega$	$R_l = 0.175\,\Omega$	$R_l = 0.12\,\Omega$	$R_l = 0.175\,\Omega$
	$L_l = 318\,\mu\text{H}$	$L_l = 1847\,\mu\text{H}$	$L_l = 318\,\mu\text{H}$	$L_l = 1847\,\mu\text{H}$

Table 3 MG loads

Load 1	Load 2	Load 3	Load 4	Load 5
$R = 300\,\Omega$	$R = 40\,\Omega$	$R = 50\,\Omega$	$R = 40\,\Omega$	$R = 50\,\Omega$
$L = 477\,\mu\text{H}$	$L = 64\,\text{mH}$	$L = 64\,\text{mH}$	$L = 64\,\text{mH}$	$L = 95\,\text{mH}$

(34) are activated at $t = 1.5\,\text{s}$, i.e. stage 2, the voltage and frequency quickly synchronise to their nominal values $V_{\text{nom}} = 380\,\text{V}$, and $f_{\text{nom}} = (\omega_{\text{nom}}/2 * \pi) = 50\,\text{Hz}$, respectively, within 0.23 s. Further, the proposed secondary synchronisation schemes are effective when the RL load of $R = 30\,\Omega$, $L = 47\,\text{mH}$ is connected to load 1 at $t = 2.5\,\text{s}$. It is clear from Fig. 4 that the proposed controller achieves consensus against the inclusion of load and precisely synchronises the voltage and frequency of MG. Next, at $t = 3.5\,\text{s}$, load 3 is removed from the MG. The proposed synchronisation scheme can restore the voltage and frequency with small transient within 0.25 s.

4.2 Case 2: Communication topology changes

In this case, we verify the performance of the proposed controller with a change in communication topology. The topology used in this case is shown in Fig. 3*b*. The design specification of the controller is similar to case 1. Fig. 5 shows that, with different communication topology, the proposed secondary controller works properly and synchronises the voltage and frequency of the islanded MG to their nominal values within 0.25 s.

4.3 Case 3: Comparison of the proposed controller with the method in [17]

As mentioned in the introduction, limited studies were reported that deal with both the voltage and frequency synchronisation in a distributed manner. [17, 18], have considered the related problems. However, in [18], only frequency restoration has been considered. Therefore, we compared the proposed controller with the controller reported in [17] for the same MG test system shown in Fig. 6. The MG parameters are taken the same for both the approaches. Fig. 6 shows that the proposed control scheme performs more accurately despite changes happen in a load and communication topology. The proposed method takes less time to synchronise the voltage and frequency compared to the method reported in [17].

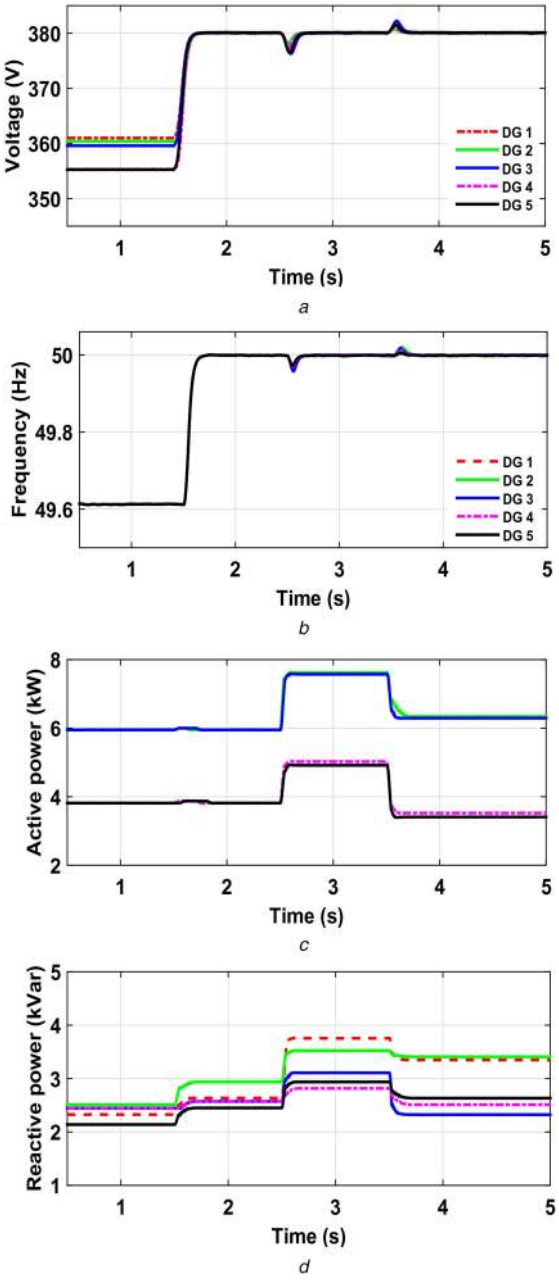

Fig. 4 *Performance evaluation for case 1*
a DG output voltage magnitude
b DG frequency
c DG output active power
d DG output reactive power

4.4 Case 4: Effect of communication latency

Communication plays an important role in preparing a framework that permits the information exchange among various elements of the MG. The influence of communication increases when a consensus algorithm is used for the secondary control layer of the MG. In this case study, the effect of communication delay on the proposed control approach is illustrated under three cases, fix communication delay of $\tau_d = 0.1, 1$ and $2\,\text{s}$ in the MG. The voltage and frequency deviate at $t = 0.5$ and $1\,\text{s}$ when loads 1 and 4 increased, respectively. At $t = 1.5\,\text{s}$, the secondary control is activated, and the restoration process starts for all DG units. For simplicity, only the voltage and frequency responses of one DG unit are given for the three different delays as shown in Figs. 7 and 8. It can be seen from Figs. 7*a* and *b* that the controller works accurately with a small time delay of 0.1 s. Figs. 7*c* and *d* show that when the time delay τ_d is increased to 1 s, the voltage/frequency is restored after a small deviation but the convergence time is increased. Further, when the delay continues to increase to

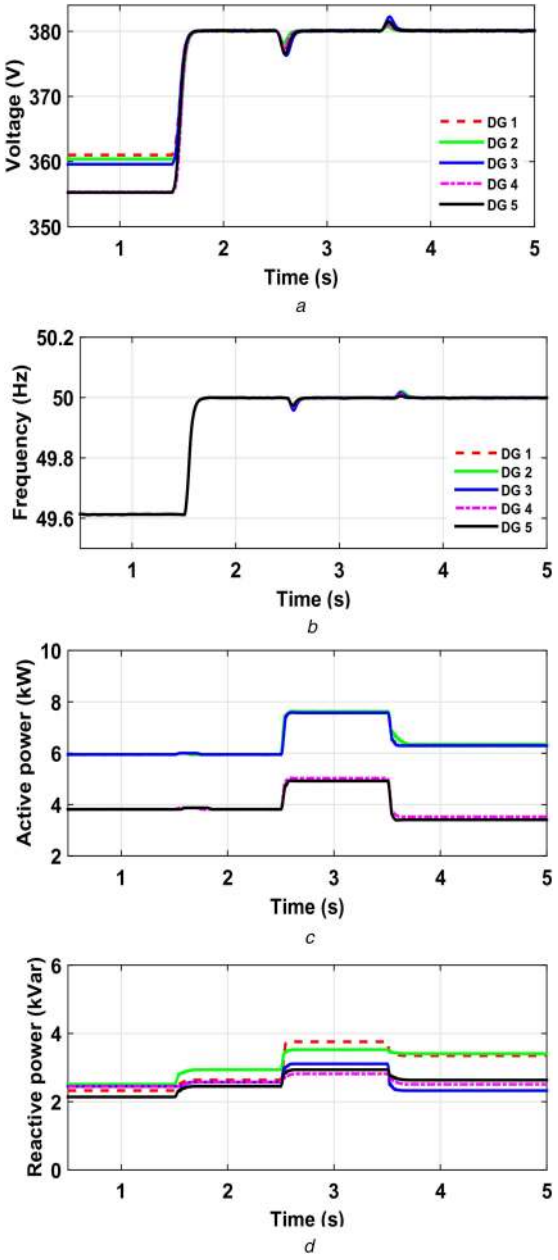

Fig. 5 *Performance evaluation for case 2*
a DG output voltage magnitude
b DG frequency
c DG output active power
d DG output reactive power

2 s, the proposed controller restores the voltage/frequency, but with more convergence time as shown in Fig. 8. Thus, it can be summarised that the communication latency can delay the convergence rate of the controller.

4.5 Case 5: Algorithm verification with a modified IEEE 39-bus system

To test the scalability, in this case, we analyse the performance of the proposed restoration algorithm for the modified IEEE-39 bus system. It consists of ten DG units and the topology and specifications are provided in [43]. Before $t = 2$ s only primary droop control was active which results in voltage and frequency deviations. The proposed control algorithm was activated at $t = 2$ s to restore the voltage and frequency to their nominal values. As shown in Fig. 9, the voltage, and frequency of all DGs are restored to 50 Hz within 0.28 s. This verifies the efficacy of the proposed restoration algorithm for more number of DG units.

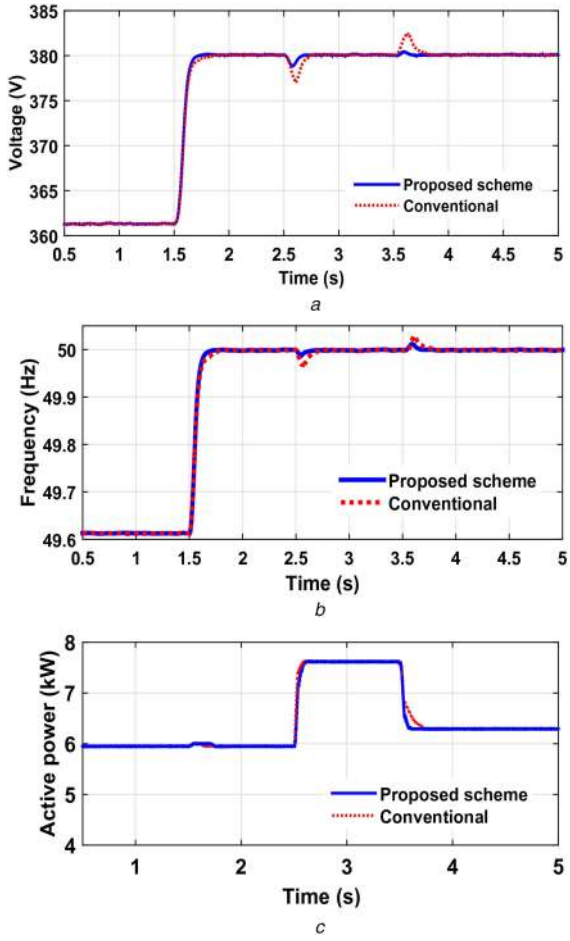

Fig. 6 *Performance comparison of the proposed scheme and the controller in [17]*
a DG output voltage magnitude
b DG frequency
c DG output active power

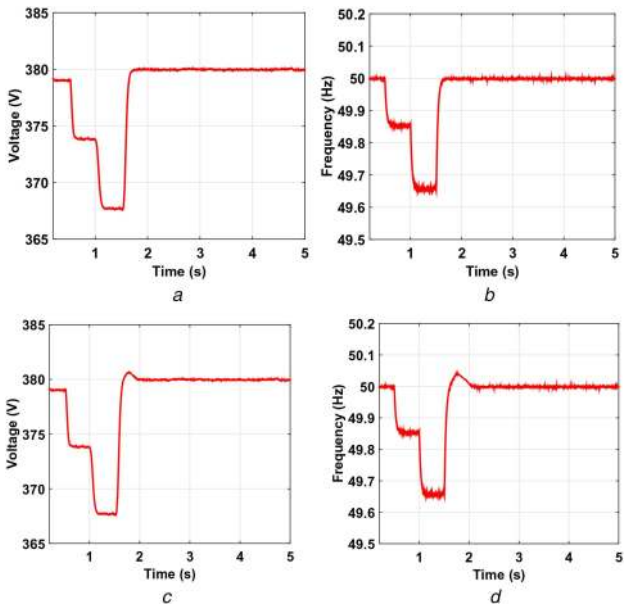

Fig. 7 *Effect of communication delay*
a DG output voltage magnitude for delay $\tau_d = 0.1$ s
b DG frequency for delay $\tau_d = 0.1$ s
c DG output voltage magnitude for delay $\tau_d = 1$ s
b DG frequency for delay $\tau_d = 1$ s

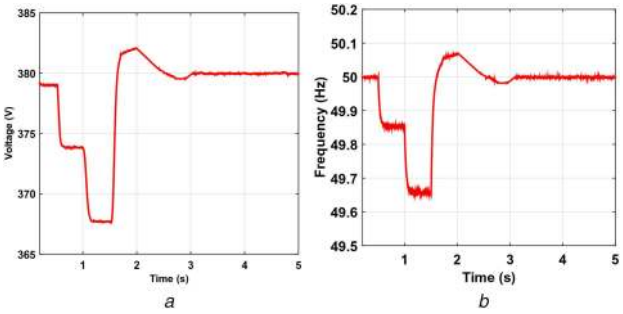

Fig. 8 *Effect of communication delay for* $\tau_d = 2\,\text{s}$
a DG output voltage magnitude
b DG frequency

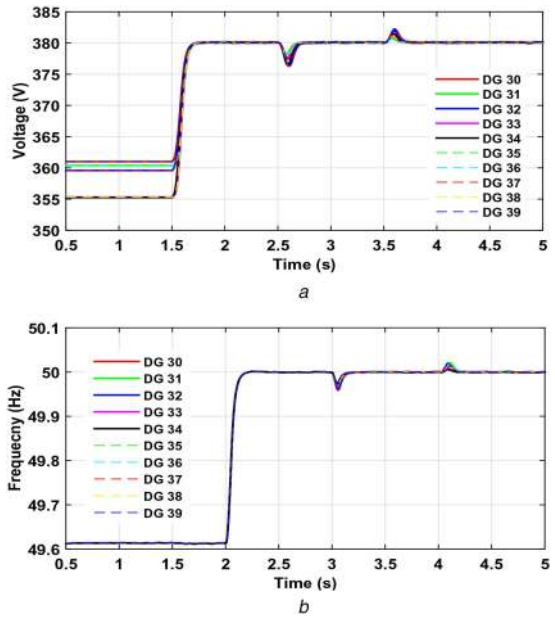

Fig. 9 *Performance for IEEE 39-bus system*
a DG output voltage magnitude
b DG frequency

4.6 Case 6: Plug-and-play (PNP) operation

In this case, the PNP functionality of the proposed restoration algorithm is investigated. DG 5 is disconnected at $t = 3\,\text{s}$ and then reconnected at $t = 4\,\text{s}$. The system parameters remain the same as given in Tables 1–3. As shown in Fig. 10, when DG 5 is disconnected at $t = 3\,\text{s}$ the remaining active DGs in MG network manages to supply the loads. It can be observed from Figs. 10*c* and *d* that the active and reactive power output of DG 5 slowly drops to zero due to the filter of DG 5. The voltage stability and frequency stability are maintained with minimal transients. At $t = 4\,\text{s}$, DG 5 is reconnected in the MG and the voltage, frequency and power regulation are maintained seamlessly, hence the proposed restoration algorithm supports the PNP capability of MG.

5 Conclusion

This paper deals with the problem of voltage and frequency synchronisation in an islanded MG scenario. A distributed secondary control scheme is proposed for both voltage and frequency synchronisation. The stability and convergence analysis for the proposed scheme have been pursued to analyse the convergence. The MG is modelled as a multi-agent system, and the DG units share information with neighbouring DG's over and sparse communication network. Unlike the centralised control structure, the proposed method is fully distributed; hence it overcomes the risk of single point failure and increases the system reliability. The effectiveness of the proposed method has been verified with extensive simulation studies in MATLAB/SimPowersystem environment. The results obtained envisage that

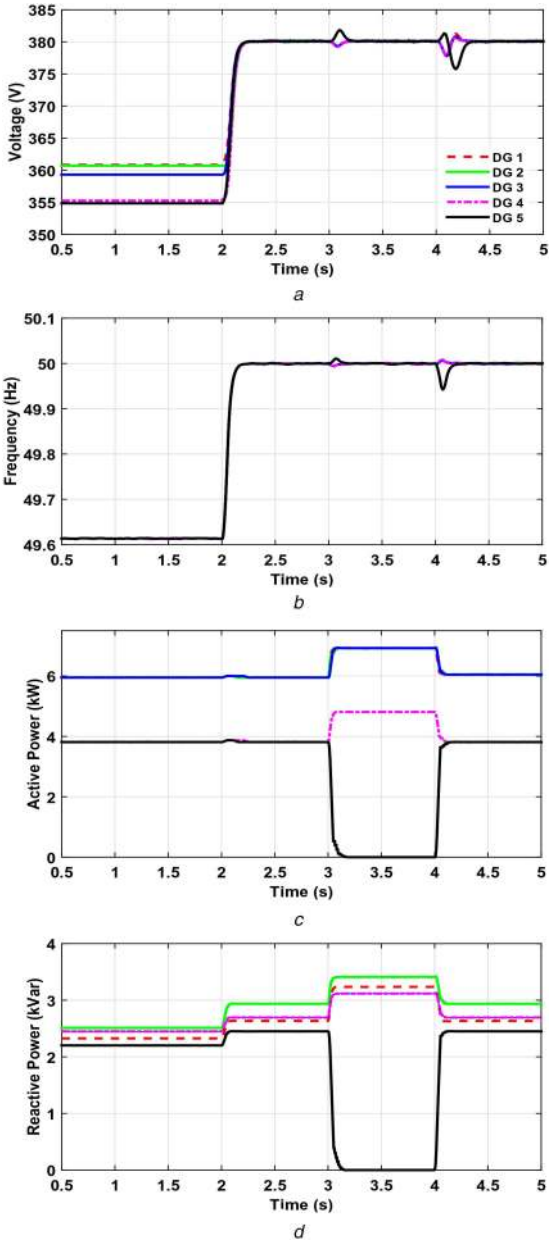

Fig. 10 *Performance under PNP operation*
a DG output voltage magnitude
b DG frequency
c DG output active power
d DG output reactive power

the proposed control scheme restores the voltage and frequency of the overall system quickly with the inclusion or removal of load and with the changing communication topology in the islanded MG. Further, the effect of communication latency, disconnection, and reconnection of DG unit and scalability on the proposed control is investigated. The proposed control strategy can withstand a delay of 2 s, and also supports PNP and scalability operation.

6 References

[1] Hatziargyriou, N., Asano, H., Iravani, R., *et al.*: 'Microgrids', *IEEE Power Energy Mag.*, 2007, **5**, (4), pp. 78–94
[2] Lasseter, R.H.: 'Microgrids'. Power Engineering Society Winter Meeting, New York, USA, 2002, vol. **1**, pp. 305–308
[3] Farhangi, H.: 'The path of the smart grid', *IEEE Power Energy Mag.*, 2010, **8**, (1), pp. 18–28
[4] Green, T., Prodanović, M.: 'Control of inverter-based micro-grids', *Electr. Power Syst. Res.*, 2007, **77**, (9), pp. 1204–1213
[5] Katiraei, F., Iravani, R., Hatziargyriou, N., *et al.*: 'Microgrids management', *IEEE Power Energy Mag.*, 2008, **6**, (3), pp. 54–65
[6] Lopes, J.P., Moreira, C., Madureira, A.: 'Defining control strategies for microgrids islanded operation', *IEEE Trans. Power Syst.*, 2006, **21**, (2), pp. 916–924

[7] Guerrero, J.M., Vasquez, J.C., Matas, J., *et al.*: 'Hierarchical control of droop-controlled ac and dc microgrids a general approach toward standardization', *IEEE Trans. Ind. Electron.*, 2011, **58**, (1), pp. 158–172

[8] Guerrero, J.M., Chandorkar, M., Lee, T.L., *et al.*: 'Advanced control architectures for intelligent microgrids – Part i: decentralized and hierarchical control', *IEEE Trans. Ind. Electron.*, 2013, **60**, (4), pp. 1254–1262

[9] Vasquez, J.C., Guerrero, J.M., Miret, J., *et al.*: 'Hierarchical control of intelligent microgrids', *IEEE Ind. Electron. Mag.*, 2010, **4**, (4), pp. 23–29

[10] Bidram, A., Davoudi, A.: 'Hierarchical structure of microgrids control system', *IEEE Trans. Smart Grid*, 2012, **3**, (4), pp. 1963–1976

[11] Guerrero, J.M., Loh, P.C., Lee, T.L., *et al.*: 'Advanced control architectures for intelligent microgrids – Part ii: power quality, energy storage, and ac/dc microgrids', *IEEE Trans. Ind. Electron.*, 2013, **60**, (4), pp. 1263–1270

[12] Parlak, K.S., Özdemir, M., Aydemir, M.T.: 'Active and reactive power sharing and frequency restoration in a distributed power system consisting of two ups units', *Int. J. Electr. Power Energy Syst.*, 2009, **31**, (5), pp. 220–226

[13] Xin, H., Qu, Z., Seuss, J., *et al.*: 'A self-organizing strategy for power flow control of photovoltaic generators in a distribution network', *IEEE Trans. Power Syst.*, 2011, **26**, (3), pp. 1462–1473

[14] Li, Z., Duan, Z., Chen, G., *et al.*: 'Consensus of multiagent systems and synchronization of complex networks: a unified viewpoint', *IEEE Trans. Circuits Syst. I, Regul. Pap.*, 2010, **57**, (1), pp. 213–224

[15] Guo, F., Wen, C., Mao, J., *et al.*: 'Distributed secondary voltage and frequency restoration control of droop-controlled inverter-based microgrids', *IEEE Trans. Ind. Electron.*, 2015, **62**, (7), pp. 4355–4364

[16] Savaghebi, M., Jalilian, A., Vasquez, J.C., *et al.*: 'Secondary control scheme for voltage unbalance compensation in an islanded droop-controlled microgrid', *IEEE Trans. Smart Grid*, 2012, **3**, (2), pp. 797–807

[17] Bidram, A., Davoudi, A., Lewis, F.L., *et al.*: 'Secondary control of microgrids based on distributed cooperative control of multi-agent systems', *IET Gener. Transm. Distrib.*, 2013, **7**, (8), pp. 822–831

[18] Bidram, A., Davoudi, A., Lewis, F.L., *et al.*: 'Distributed cooperative secondary control of microgrids using feedback linearization', *IEEE Trans. Power Syst.*, 2013, **28**, (3), pp. 3462–3470

[19] Schiffer, J., Seel, T., Raisch, J., *et al.*: 'Voltage stability and reactive power sharing in inverter-based microgrids with consensus-based distributed voltage control', *IEEE Trans. Control Syst. Technol.*, 2016, **24**, (1), pp. 96–109

[20] Cady, S.T., Domnguez Garca, A.D.: 'Distributed generation control of small-footprint power systems'. North American Power Symp. (NAPS), Champaign, IL, USA, 2012, pp. 1–6

[21] Simpson Porco, J.W., Dörfler, F., Bullo, F.: 'Synchronization and power sharing for droop-controlled inverters in islanded microgrids', *Automatica*, 2013, **49**, (9), pp. 2603–2611

[22] Bidram, A., Davoudi, A., Lewis, F.L.: 'A multiobjective distributed control framework for islanded ac microgrids', *IEEE Trans. Ind. Inf.*, 2014, **10**, (3), pp. 1785–1798

[23] Nasirian, V., Shafiee, Q., Guerrero, J.M., *et al.*: 'Droop-free distributed control for ac microgrids', *IEEE Trans. Power Electron.*, 2016, **31**, (2), pp. 1600–1617

[24] Simpson Porco, J.W., Dorfler, F., Bullo, F., *et al.*: 'Stability, power sharing, & distributed secondary control in droop-controlled microgrids'. 2013 IEEE Int. Conf. on Smart Grid Communications (SmartGridComm), Vancouver, BC, Canada, 2013, pp. 672–677

[25] Shafiee, Q., Nasirian, V., Guerrero, J.M., *et al.*: 'Team-oriented adaptive droop control for autonomous ac microgrids'. 40th Annual Conf. of the IEEE Industrial Electronics Society, IECON 2014, Dallas, TX, USA, 2014, pp. 1861–1867

[26] Yazdanian, M., Mehrizi Sani, A.: 'Distributed control techniques in microgrids', *IEEE Trans. Smart Grid*, 2014, **5**, (6), pp. 2901–2909

[27] Olfati Saber, R., Murray, R.M.: 'Consensus problems in networks of agents with switching topology and time-delays', *IEEE Trans. Autom. Control*, 2004, **49**, (9), pp. 1520–1533

[28] Ahumada, C., Cárdenas, R., Sáez, D., *et al.*: 'Secondary control strategies for frequency restoration in islanded microgrids with consideration of communication delays', *IEEE Trans. Smart Grid*, 2016, **7**, (3), pp. 1430–1441

[29] Zhang, W., Xu, Y., Liu, W., *et al.*: 'Fully distributed coordination of multiple dfigs in a microgrid for load sharing', *IEEE Trans. Smart Grid*, 2013, **4**, (2), pp. 806–815

[30] Xu, Y., Zhang, W., Liu, W., *et al.*: 'Distributed subgradient-based coordination of multiple renewable generators in a microgrid', *IEEE Trans. Power Syst.*, 2014, **29**, (1), pp. 23–33

[31] Shafiee, Q., Guerrero, J.M., Vasquez, J.C.: 'Distributed secondary control for islanded microgrids-a novel approach', *IEEE Trans. Power Electron.*, 2014, **29**, (2), pp. 1018–1031

[32] Shafiee, Q., Nasirian, V., Vasquez, J.C., *et al.*: 'A multi-functional fully distributed control framework for ac microgrids', *IEEE Trans. Smart Grid*, 2016, **9**, (4), pp. 3247–3258

[33] Dehkordi, N.M., Sadati, N., Hamzeh, M.: 'Fully distributed cooperative secondary frequency and voltage control of islanded microgrids', *IEEE Trans. Energy Convers.*, 2017, **32**, (2), pp. 675–685

[34] Pogaku, N., Prodanovic, M., Green, T.C.: 'Modeling, analysis and testing of autonomous operation of an inverter-based microgrid', *IEEE Trans. Power Electron.*, 2007, **22**, (2), pp. 613–625

[35] Shrivastava, S., Subudhi, B., Das, S.: 'Voltage and frequency synchronization of a low voltage inverter based microgrid'. 4th Int. Conf. on Power, Control & Embedded Systems (ICPCES), Allahabad, 9–11 March 2017, pp. 1–6

[36] Zuo, S., Davoudi, A., Song, Y., *et al.*: 'Distributed finite-time voltage and frequency restoration in islanded ac microgrids', *IEEE Trans. Ind. Electron.*, 2016, **63**, (10), pp. 5988–5997

[37] Rocabert, J., Luna, A., Blaabjerg, F., *et al.*: 'Control of power converters in ac microgrids', *IEEE Trans. Power Electron.*, 2012, **27**, (11), pp. 4734–4749

[38] Lou, G., Gu, W., Xu, Y., *et al.*: 'Distributed mpc-based secondary voltage control scheme for autonomous droop-controlled microgrids', *IEEE Trans. Sustain. Energy*, 2017, **8**, (2), pp. 792–804

[39] Moradi, M.H., Eskandari, M., Hosseinian, S.M.: 'Cooperative control strategy of energy storage systems and micro sources for stabilizing microgrids in different operation modes', *Int. J. Electr. Power Energy Syst.*, 2016, **78**, pp. 390–400

[40] Shrivastava, S., Subudhi, B., Das, S.: 'Consensus-based voltage and frequency restoration scheme for inertia-less islanded microgrid with communication latency'. Region 10 Conf., TENCON, Penang, 21–24 November 2017, pp. 745–750

[41] Qu, Z., Wang, J., Hull, R.A.: 'Cooperative control of dynamical systems with application to autonomous vehicles', *IEEE Trans. Autom. Control*, 2008, **53**, (4), pp. 894–911

[42] Kia, S.S., Cortés, J., Martinez, S.: 'Dynamic average consensus under limited control authority and privacy requirements', *Int. J. Robust Nonlinear Control*, 2015, **25**, (13), pp. 1941–1966

[43] Zhao, T., Ding, Z.: 'Distributed finite-time optimal resource management for microgrids based on multi-agent framework', *IEEE Trans. Ind. Electron.*, 2017, **65**, (8), pp. 6571–6580